HUMAN GENE THERAPY 19:579–588 (June 2008)

DOI: 10.1089/hum.2007.168

Biochemical Correction of Short-Chain Acyl-Coenzyme A Dehydrogenase Deficiency After Portal Vein Injection of rAAV8-SCAD

Stuart G. Beattie,[1] Eric Goetzman,[2] Thomas Conlon,[3] Sean Germain,[3] Glenn Walter,[3] Martha Campbell-Thompson,[3] Dietrich Matern,[4] Jerry Vockley,[2] and Terence R. Flotte[1]

Abstract

Recombinant adeno-associated viral vectors pseudotyped with serotype 5 and 8 capsids (AAV5 and AAV8) have been shown to be efficient gene transfer reagents for the liver. We have produced AAV5 and AAV8 vectors that express mouse short-chain acyl-CoA dehydrogenase (mSCAD) cDNA under the transcriptional control of the cytomegalovirus–chicken β-actin hybrid promoter. We hypothesized that these vectors would produce sufficient hepatocyte transduction (after administration via the portal vein) and thus sufficient SCAD enzyme to correct the phenotype observed in the SCAD-deficient (BALB/cByJ) mouse, which includes elevated blood butyrylcarnitine and hepatic steatosis. Ten weeks after portal vein injection into 8-week-old mice, AAV8-treated livers contained acyl-CoA dehydrogenase activity (14.3 mU/mg) toward butyryl-CoA, compared with 7.6 mU/mg in mice that received phosphate-buffered saline. Immunohistochemistry showed expression of mSCAD within rAAV8-mSCAD-transduced hepatocytes, as seen by light microscopy. A significant reduction of circulating butyrylcarnitine was seen in AAV5-mSCAD- and AAV8-mSCAD-injected mice. Magnetic resonance spectroscopy of fasted mice demonstrated a significant reduction in relative lipid content within the livers of AAV8-mSCAD-treated mice. These results demonstrate biochemical correction of SCAD deficiency after AAV8-mediated SCAD gene delivery.

Introduction

MITOCHONDRIAL FATTY ACID OXIDATION is the primary source of energy for heart and slow-twitch skeletal muscle. Moreover, during prolonged fasting or physiological stress, β-oxidation of fatty acids in the liver generates ketone bodies that supply energy for the brain, muscles, and other organs. Mitochondrial catabolism of fatty acids occurs by repeated cycling through a four-step β-oxidation spiral, with each round producing one molecule of $FADH_2$, one of NADH, and one of acetyl-CoA. Inborn errors of metabolism affecting this pathway are typically inherited in a recessive fashion. Affected individuals deficient for medium- and very long-chain acyl-CoA dehydrogenase (MCAD and VLCAD, respectively) may present with heart and skeletal muscle dysfunction, nonketotic hypoglycemia, or sudden infant death syndrome. Postmortem histological findings almost always include organ lipidosis (Rinaldo and Matern, 2005).

The first step in the β-oxidation spiral is rate-limiting and is catalyzed by a family of acyl-CoA dehydrogenases (ACADs) that differ in their substrate specificity based on the carbon chain length of the fatty acid. Short-chain acyl-CoA dehydrogenase (SCAD; OMIM [Online Mendelian Inheritance in Man; see http://www.ncbi.nlm.nih.gov/sites/entrez?db=omim] 606885) is specific for acyl-CoAs four to six carbons in length (Naito *et al.*, 1989). SCAD deficiency (SCADD, OMIM 201470) is a heterogeneous condition that has been associated with various clinical phenotypes ranging from fatal metabolic decompensation in infancy, developmental delay, hyper- and hypotonia, seizures, ketotic hypoglycemia, to late-onset progressive myopathy (Bhala *et al.*, 1995; van Maldegem *et al.*, 2006; Tein *et al.*, 2008). Some individuals with biochemically apparent SCADD remain asymptomatic (Ribes *et al.*, 1998), making it impossible to differentiate diseased from nondiseased individuals (van Maldegem *et al.*, 2006), and the most common presentation

[1]University of Massachusetts Medical School, Worcester, MA 01655.
[2]Department of Pediatrics, University of Pittsburgh School of Medicine and Children's Hospital of Pittsburgh, Pittsburgh, PA 15123.
[3]Powell Gene Therapy Center, University of Florida, Gainesville, FL 32610.
[4]Department of Laboratory Medicine and Pathology, Mayo Clinic College of Medicine, Rochester, MN 55905.

of SCADD is asymptomatic. When SCAD activity is impaired, butyryl-CoA (C_4-CoA) accumulates along with the corresponding carnitine ester (butyrylcarnitine), the corresponding glycine ester (butyrylglycine), butyrate, and ethylmalonic acid (EMA). SCADD can be defined by the presence of elevated butyrylcarnitine in blood and/or increased EMA levels in urine under nonstressed conditions (van Maldegem *et al*., 2006).

Twenty-two rare mutations have been reported in the SCAD gene (*ACADS*), nearly all of which are missense mutations, leading to complete inactivation of SCAD activity (Naito *et al*., 1990; Gregersen *et al*., 1998; Corydon *et al*., 2001; Seidel *et al*., 2003; van Maldegem *et al*., 2006). The two common SCAD gene variants 625G → A (Gly185Ser) and 511C → T (Arg147Trp) are polymorphic in the Western European population and encode proteins with decreased catalytic activity and/or thermostability (Gregersen *et al*., 1998; Corydon *et al*., 2001). van Maldegem and coworkers (2006) calculated that a birth prevalence of at least 1:50,000 in the Netherlands occurs for SCADD, indicating that SCADD is far more common than previously assumed (Nagan *et al*., 2003).

SCAD-deficient ($SCAD^{-/-}$) BALB/cByJ mice have a spontaneous deletion of 278 nucleotides at the 3′ end of the SCAD gene, resulting in a phenotype similar to the human deficiency, with elevated levels of butyrylcarnitine, organic aciduria, and accumulation of lipid droplets within liver and muscle (Armstrong *et al*., 1993; Kelly *et al*., 1997). Mitochondrial swelling and microvesicular fatty changes in hepatocytes have been observed in this mouse model, especially severe after a fast. Increased levels of circulating fatty acids infiltrate the liver in response to fasting, when they would act as the primary source of energy. Unless stressed by fasting and/or cold, the life span of these mice appears normal. Indeed, the $SCAD^{-/-}$ mouse is a somewhat limited model and does not display any clinical manifestations. However, it does act as a surrogate model for human SCAD, MCAD, and VLCAD deficiencies.

Liver-directed gene expression of the wild-type SCAD cDNA by the hydrodynamic gene delivery method has been reported by Holm and coworkers (2003). SCAD enzyme activity in $SCAD^{-/-}$ mice was undetectable after 2 weeks and the butyrylcarnitine profile was not normalized. Delivery of the murine SCAD cDNA has previously been demonstrated in our laboratory, using a recombinant adeno-associated virus serotype 1 (AAV1) vector carrying the murine SCAD cDNA (Conlon *et al*., 2006). Ten weeks postinjection into the tibialis anterior (TA) muscle of $SCAD^{-/-}$ mice, SCAD enzyme activity was detected and the levels of circulating butyrylcarnitine were significantly reduced. Magnetic resonance spectroscopy demonstrated a reduction of the lipid peak in injected TA muscle. In the present studies we investigated the benefits of liver-directed gene replacement for SCAD deficiency. Thus, AAV5 and AAV8 vectors were evaluated for their potential toward efficient delivery and stable expression of mSCAD in the SCAD-deficient mouse model.

Materials and Methods

Producing and purifying recombinant AAV vectors

The University of Florida Powell Gene Therapy Center (Gainesville, FL) produced recombinant adeno-associated virus with pseudotype 5 and 8 capsids for these studies. The AAV recombinant genome, pCB-mSCAD, contains the coding sequence for murine SCAD under the transcriptional control of the cytomegalovirus enhancer/chicken β-actin promoter (Xu *et al*., 2001). Virus production included use of the helper/packaging plasmids pXY5 and pDG8, for rAAV5 and rAAV8, respectively, which supply all the necessary helper functions as well as Rep and Cap proteins *in trans*. Vector plasmid (622.5 μg) pCB-mSCAD was cotransfected by calcium phosphate precipitation with 1867 μg of pDG8 into a single cell factory (632-cm^2 surface area; Nunc, Rochester, NY) of ~70–95% confluent 293 cells. Recombinant AAV was purified by iodixanol step gradient centrifugation and HiTrap Q-Sepharose ion-exchange column purification (GE Healthcare, Piscataway, NJ). Biomax 100K cutoff filters were used to desalt and concentrate rAAV (Millipore, Billerica, MA). Vector titers were determined by dot-blot assay as described (Zolotukhin *et al*., 2002), with 6.7×10^{12} genome copies/ml for AAV5-mSCAD and 1.6×10^{13} genome copies/ml for AAV8-mSCAD. Standard assays for the infectivity of rAAV5 and rAAV8 are not available, so the genome copy-to-infectivity ratio was not determined.

Animals

BALB/cByJ mice with a homozygous natural deletion of the endogenous SCAD gene (Wood *et al*., 1989) were purchased from Jackson Laboratories (Bar Harbor, ME). Mice were maintained in plastic cages in pathogen-free facilities with a 12-hr light and 12-hr dark cycle. Mice were fed a standard chow and watered *ad libitum*. All animal surgeries and care were approved by the University of Florida Institutional Animal Care and Use Committee in accordance with Association for Assessment and Accreditation of Laboratory Animal Care International specifications. Mice were fasted overnight before magnetic resonance spectroscopy scanning and before tissue collection on sacrifice. Of note, the ideal control mouse, BALB/cBy, was available only as an embryonic stock at the time of experimentation. Previous experiments in our laboratory have demonstrated comparable butyrylcarnitine levels in both BALB/cBy and C57BL/6 strains containing an intact SCAD sequence.

Portal vein injection

Ten 8-week-old female $SCAD^{-/-}$ mice were injected via the hepatic portal vein with 1×10^{11} vector genomes (vg) each. Ten mice received phosphate-buffered saline (PBS), acting as the negative control group. Mice were randomly assigned to both treatment groups. To perform the portal vein injections, all animals were anesthetized with 3% isoflurane. A ventral midline abdominal incision was made into the peritoneal cavity, and the portal vein was exposed. AAV vector or PBS (30 μl) was administered into the portal vein with a 31-gauge BD insulin syringe with BD Ultra-Fine II short needle (Becton Dickinson, Franklin Lakes, NJ). Hemostasis was achieved by application of a cotton fiber tipped sterile swab directly onto the site of injection into the portal vein. Surgeries were performed on a thermoregulated operating board designed to maintain a temperature of 37°C throughout the procedure, which routinely took 20 min to perform. To determine the concentration of circulating butyrylcarnitines,

serum samples were obtained via the tail vein at regular intervals (0, 2, 4, 6, 8, and 10 weeks postinjection). At 10 weeks after rAAV administration, mice were killed by anesthetization with 5% isoflurane followed by cervical dislocation.

Immunohistochemistry

The liver was completely removed. Sections from two or three hepatic lobes were frozen in a mixture of isopentane and dry ice for subsequent mitochondrial isolation or fixed in 10% neutral-buffered formalin for histology and immunohistochemistry. Formalin-fixed, paraffin-embedded tissue sections (4 μm) were sequentially deparaffinized, blocked for endogenous peroxidase activity with 3% hydrogen peroxidase in methanol for 10 min, and rehydrated. Slides were subsequently rinsed in 1× Dako wash buffer (1× PBS with 0.05% Tween; Dako, Glostrup, Denmark) and incubated with a universal protein blocker, Background Sniper (Biocare Medical, Concord, CA), for 15 min and rinsed again in 1× Dako wash buffer, before a 1-hr incubation with either rabbit anti-rat SCAD or normal rabbit immunoglobulin as a negative control. The rabbit anti-rat SCAD antibody was supplied as rabbit serum by the laboratory of one of the authors (J. Vockley, Department of Pediatrics, University of Pittsburgh School of Medicine, Pittsburgh, PA), and was purified with a 1-ml HiTrap protein G HP column (GE Healthcare Life Sciences, Piscataway, NJ). The purified rabbit anti-rat SCAD antibody was diluted 1:3000. Slides were rinsed for 5 min followed by incubation in MACH 2 rabbit horseradish peroxidase (HRP) polymer (Biocare Medical) for 30 min at room temperature. Detection of SCAD was achieved by incubating slides in Cardassian 3,3′-diaminobenzidine (DAB) (Biocare Medical) for 5 min at room temperature. Slides were counterstained with hematoxylin (Vector Laboratories, Burlingame, CA) and mounted. Representative digital images were captured with a Zeiss Axioskop equipped with an Axiocam camera (Carl Zeiss, Oberkochen, Germany). Camera exposure settings were constant for all images.

Western blotting

Mitochondrial protein was extracted from 30 mg of liver, using a mitochondria isolation kit (MITOISO1; Sigma-Aldrich, St. Louis, MO) as per the manufacturer's instructions for isolation from soft tissue. Fifty micrograms of mitochondrial protein from each mouse was heat-denatured and resolved by electrophoresis on a 10% Criterion sodium dodecyl sulfate (SDS)–polyacrylamide gel (Bio-Rad, Hercules, CA). Ten nanograms of pure human SCAD served as a positive control. Separated proteins were transferred to 0.2-μm Optitran nitrocellulose membrane (Whatman, Florham Park, NJ), using a TE42 Protein Transfer Tank (Hoefer Scientific Instruments, San Francisco, CA). SCAD antigen was detected with rabbit anti-rat SCAD antibody at a 1:1000 dilution followed by a 1:3000 dilution of alkaline phosphatase-conjugated goat anti-rabbit IgG and visualization with a nitroblue tetrazolium/5-bromo-4-chloro-3-indolyl phosphate color development solution according to the manufacturer's instructions (Bio-Rad). Duplicate gels were blotted with rabbit anti-porcine MCAD antibody to demonstrate equal loading. Ten nanograms of pure human MCAD served as a positive control.

SCAD enzyme activity determination

SCAD enzyme activity in liver homogenates was measured essentially as described (Conlon *et al*., 2006). First, flash-frozen tissue pieces were homogenized for 30 sec in 600 μl of 50 m*M* Tris-HCl, pH 8.0, supplemented with 2 m*M* EDTA and Halt protease inhibitor cocktail (Pierce Biotechnology, Rockford, IL). The homogenate was centrifuged at 4°C for 20 min and the supernatant was collected. Protein concentration was determined by the Bradford method (Bradford, 1976). Enzyme activity was measured in an anaerobic electron transfer flavoprotein fluorescence reduction assay (Frerman and Goodman, 1985), using an LS50B fluorescence spectrophotometer from PerkinElmer Life and Analytical Sciences (Wellesley, MA) with a heated cuvette block set to 32°C. The enzymatic reaction was started by addition of C_4-CoA (Sigma-Aldrich) to yield a final concentration of 5 μ*M*. Specific activity was calculated with 1 milliunit (mU) of activity defined as the amount of protein necessary to completely reduce 1 nmol of electron-transferring flavoprotein (ETF) in 1 min.

Electron spray ionization–tandem mass spectrometry of serum butyrylcarnitines

Acylcarnitines in serum were measured as their butyryl esters as previously described (Rinaldo and Matern, 2005).

Magnetic resonance spectroscopy of SCAD-deficient mouse livers

Magnetic resonance imaging (MRI) and magnetic resonance spectroscopy (MRS) were performed on a 4.7-T Bruker Avance spectrometer (Bruker BioSpin, Billerica, MA). The animals were anesthetized with 1.5% isoflurane (Abbot Laboratories, Abbot Park, IL) with an oxygen flow of approximately 1 liter/min. The animals were placed prone in a home-built quadrature birdcage coil and respiration used for MRS gating was monitored with a small animal monitoring and gating system (SA Instruments, Stony Brook, NY). A survey scan was conducted to visualize the liver for voxel placement. Proton spectroscopy from a 6.75-μl voxel was acquired with a volume-selective PRESS (point-resolved spectroscopy) sequence with a TR of 2000 msec and a TE of 18 msec. Data were acquired into a 6000-Hz spectral width, composed of 4096 points. Five hundred and twelve averages were used for a total scan time of 17 min. Processing of the data was conducted with XWIN-NMR (Bruker BioSpin). Area integration of the peaks for both lipid and water was determined and arbitrary units were assigned. Water peak values are constant between different mice and were used to determine a lipid-to-water ratio indicating the relative lipid content within the liver.

Statistical analysis

A Student *t* test was used to compare groups. $p < 0.05$ was considered statistically significant.

Results

Hepatocyte expression of mSCAD delivered by AAV8 persists up to at least 10 weeks postinjection, whereas AAV5 vector-mediated expression is lost

For these studies we used AAV vectors carrying the murine SCAD cDNA sequence. Eight-week-old SCAD-defi-

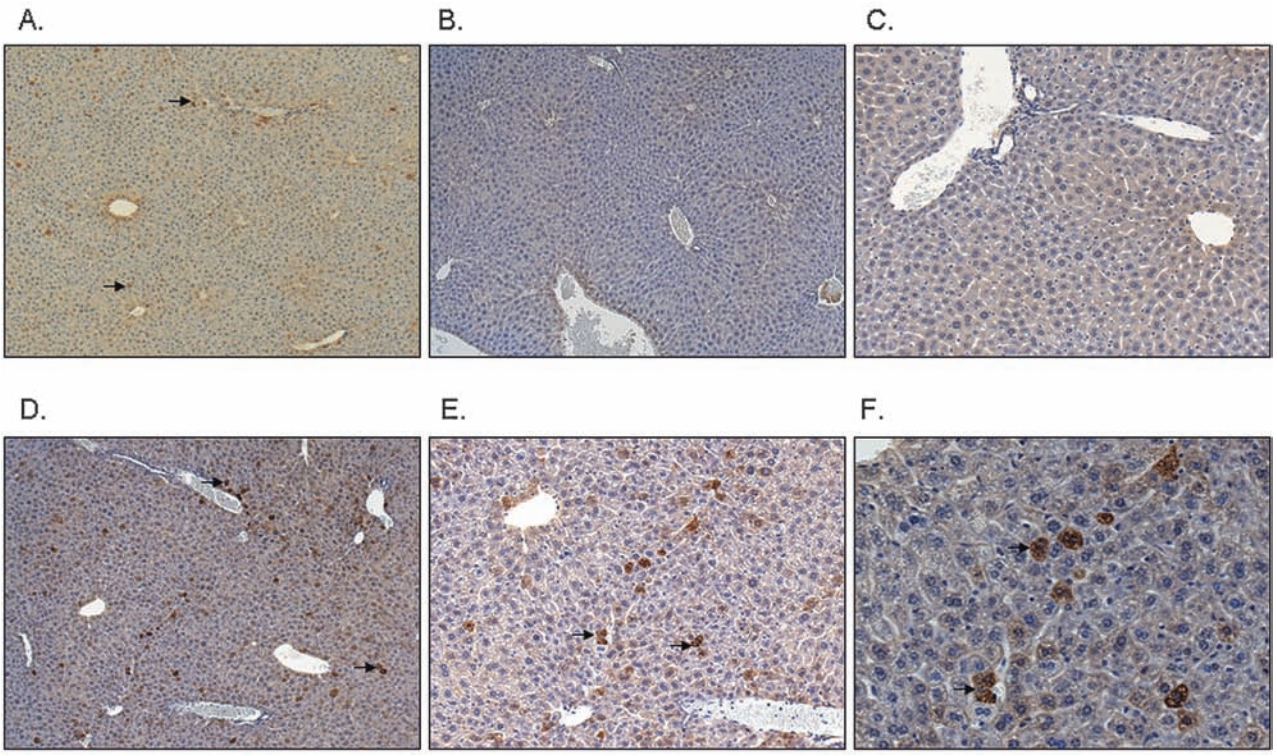

FIG. 1. Recombinant AAV8-mSCAD vector-mediated expression of murine SCAD in $SCAD^{-/-}$ liver. Sections from $SCAD^{-/-}$ mouse livers harvested 10 weeks after rAAV8-mSCAD injection were incubated with a rabbit anti-rat SCAD antibody as the primary antibody. Arrows indicate SCAD-positive hepatocytes. (**A**) C57BL/6 (wild-type) mouse liver section (original magnification, ×10). (**B** and **C**) Liver sections from $SCAD^{-/-}$ mice that received PBS via the hepatic portal vein (original magnification, ×10 and ×20, respectively). (**D–F**) Liver sections from $SCAD^{-/-}$ mice that received AAV8-mSCAD (original magnification, ×10, ×20, and ×40, respectively).

cient ($SCAD^{-/-}$) male mice were injected via the portal vein with either PBS ($n = 10$), AAV5-mSCAD ($n = 9$), or AAV8-mSCAD ($n = 9$) at a dose of 1×10^{11} vg per animal. Ten weeks postinjection livers were harvested and immunostained with a rabbit anti-rat SCAD antibody (which also recognizes murine SCAD). A wild-type ($SCAD^{+/+}$) C57BL/6 mouse liver section was included as a positive control (Fig. 1A) where, with DAB as the chromagen, there was diffuse brown staining, corresponding to endogenous SCAD protein. No SCAD protein was detectable in the PBS-treated animals (Fig. 1B and C) whereas in all mice injected with the AAV8-mSCAD vector approximately 5% of hepatocytes were estimated to have stained positive for SCAD (Fig. 1D–F). Approximately 1–2% of hepatocytes were estimated to have stained positive for SCAD 10 weeks after injection of AAV5-mSCAD (data not shown). There was no histological evidence

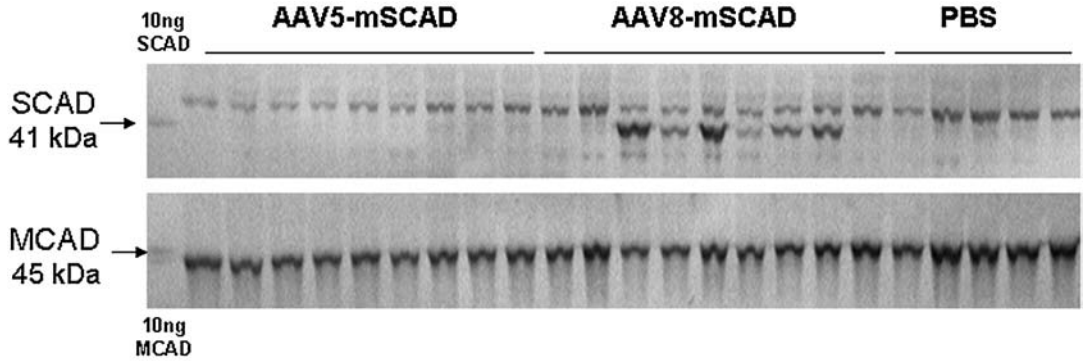

FIG. 2. SCAD protein detection in mitochondria isolated from livers of $SCAD^{-/-}$ mice 10 weeks after hepatic portal vein injection of PBS, AAV5-mSCAD, or AAV8-mSCAD. *Top*: Mitochondrial protein extracts probed with a rabbit anti-rat SCAD antibody, where 10 ng of purified human SCAD was loaded into the first lane as a positive control. *Bottom*: Mitochondrial isolates probed with a rabbit anti-porcine MCAD antibody, where 10 ng of purified human MCAD protein was loaded into the first lane as a positive control. [The anti-rat SCAD antibody cross-reacts with human and mouse SCAD protein; the anti-porcine MCAD antibody cross-reacts with human and mouse MCAD protein.]

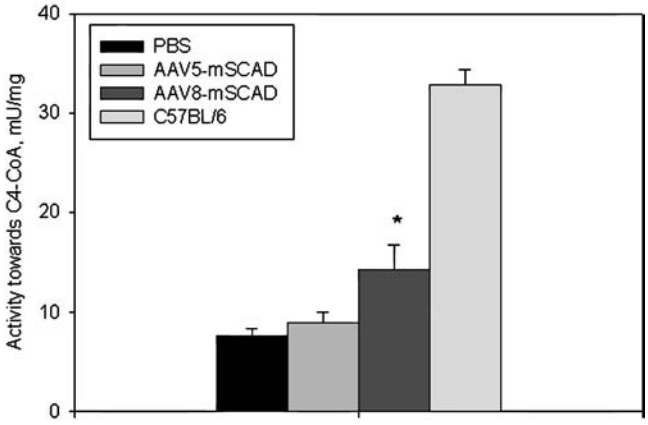

FIG. 3. SCAD enzyme activity within liver samples 10 weeks postinjection. SCAD enzyme activity was measured in crude cellular extracts from liver sections, using the anaerobic electron-transferring flavoprotein reduction assay. Columns and error bars represent means and standard errors, respectively. PBS ($n = 10$); rAAV5 ($n = 9$); rAAV8 ($n = 9$); C57BL/6 ($n = 5$). *$p < 0.05$. C_4-CoA, butyryl-CoA.

of liver toxicity from the vector or its effects as evidenced by hematoxylin and eosin staining (data not shown).

The SCAD enzyme is encoded in the nuclear genome as a precursor containing a 24-amino acid mitochondrial targeting peptide at the amino terminus. After translation in the cytoplasm, the 44-kDa precursor protein is transported to the mitochondria, where it is then imported into the matrix, proteolytically processed to its 41-kDa mature form, and assembled into an active homotetrameric holoenzyme (168 kDa) containing one molecule of FAD per subunit (Naito *et al*., 1989). To determine whether the AAV-delivered murine SCAD was properly targeted to the mitochondrial matrix, Western blotting was carried out on liver mitochondrial isolates. Immunoblotting was performed to determine whether AAV-mediated SCAD protein could be detected from mitochondrial isolates, 10 weeks postinjection. $SCAD^{-/-}$ mice injected with AAV8-mSCAD had detectable levels of murine SCAD present in liver mitochondria after 10 weeks. However, SCAD from AAV5-treated liver mitochondria could not be detected in mitochondrial isolates (Fig. 2). Note that the highest band in the top panel of Fig. 2 is due to cross-reactivity of the SCAD antibody with the related enzyme medium-chain acyl-CoA dehydrogenase (MCAD). The first lane of the Western blot represents 10 ng of purified human SCAD. As a control to demonstrate equal loading, a duplicate blot of the mitochondrial isolates was probed with rabbit anti-porcine MCAD antibody (Fig. 2, bottom). The first lane contains 10 ng of pure human MCAD.

Having demonstrated that SCAD protein encoded by the rAAV vector properly targets to liver mitochondria and persists for 10 weeks postinjection, we next asked whether the vector-delivered enzyme was active. SCAD enzyme activity was measured in crude liver extracts by the anaerobic electron-transferring flavoprotein (ETF) fluorescence reduction assay. This assay is highly sensitive and specific for the ACAD enzyme family. With C_4-CoA as substrate, activity in PBS-treated $SCAD^{-/-}$ mice was low but detectable (7.6 ± 2.2 mU/mg) because another ACAD family member, short/branched-chain acyl-CoA dehydrogenase (SBCAD) has minor activity toward C_4-CoA. Activity in the AAV5 vector-treated group (8.9 ± 3.3 mU/mg) was not significantly higher than background levels observed in PBS-injected mice. However, AAV8 vector-treated mice maintained an average specific SCAD enzyme activity of 14.3 ± 7.6 mU/mg in the samples of liver analyzed. These levels were statistically significant when compared with mice that received PBS (*t* test; $p = 0.015$). Wild-type, C57BL/6 mouse livers were determined to contain a SCAD activity level of 32.9 ± 3.4 mU/mg (Fig. 3). Thus, AAV8 vector-treated mice reached ~43% of active SCAD enzyme levels determined in wild-type mice. In TA muscle, there was no difference in enzyme activity between groups of $SCAD^{-/-}$ mice that received rAAV-SCAD vectors or PBS (data not shown).

Liver transduction diminishes the biochemical and physiologic effects of SCAD deficiency

Nonfasting levels of butyrylcarnitine were measured by electron spray ionization–tandem mass spectrometry (ESI-

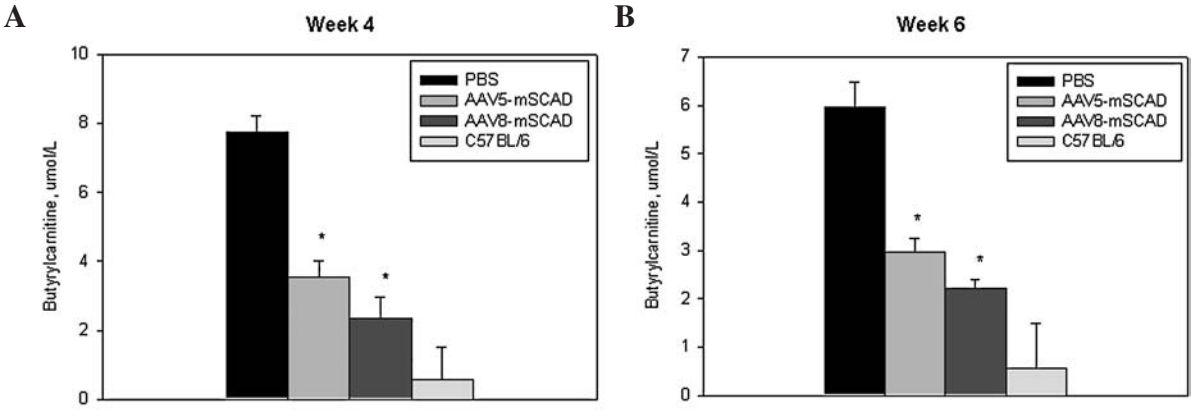

FIG. 4. Levels of circulating butyrylcarnitine in sera of $SCAD^{-/-}$ mice after injection of rAAV-mSCAD vectors via the hepatic portal vein. (**A**) Concentration of butyrylcarnitine 4 weeks postinjection. (**B**) Concentration of butyrylcarnitine 6 weeks postinjection. Columns and error bars represent means and SEs, respectively. PBS ($n = 10$); rAAV5 ($n = 9$); rAAV8 ($n = 9$); C57BL/6 ($n = 4$). *$p < 0.001$, compared with mice that received PBS.

MS/MS) in sera collected 4 and 6 weeks postadministration of rAAV vector or PBS. At 4 weeks postinjection the mean concentration of circulating butyrylcarnitine in $SCAD^{-/-}$ mice that received PBS was 7.73 ± 1.52 μmol/liter (Fig. 4A). $SCAD^{-/-}$ mice that received either AAV5 or AAV8 mSCAD vectors had significantly reduced concentrations of butyrylcarnitine (3.52 ± 1.51 and 2.36 ± 1.76 μmol/liter, respectively, with p values less than 0.001 for both, compared with PBS-treated mice). Untreated, SCAD-expressing C57BL/6 (wild-type) mice had a mean circulating butyrylcarnitine concentration of 0.57 ± 0.92 μmol/liter at 18 weeks of age (reported as part of the study in which AAV1-mSCAD vector was injected into TA muscle; see Conlon *et al.*, 2006). ESI-MS/MS performed on sera 6 weeks postinjection (Fig. 4B) determined that butyrylcarnitine levels were still significantly reduced in mice that received AAV5 or AAV8 vector (2.96 ± 0.88 and 2.20 ± 0.55 μmol/liter, respectively) compared with PBS (5.97 ± 1.59 μmol/liter). Significance (p) values were less than 0.001 for both AAV5-mSCAD- and AAV8-mSCAD-treated mice, compared with those that received PBS. The same circulating butyrylcarnitine concentration (0.57 ± 0.92 μmol/liter) was used as week 4 postinjection. The reduction in circulating butyrylcarnitine levels in mice that received rAAV-SCAD vectors compared with those that received PBS can be directly attributed to the expression of exogenous SCAD enzyme in hepatocytes. Despite circulating butyrylcarnitine levels in rAAV-SCAD-treated mice not decreasing to $SCAD^{+/+}$ levels observed in C57BL/6 mice, there is a clear trend toward wild-type levels. Circulating blood glucose concentrations in fasted $SCAD^{-/-}$ mice were measured and showed no difference between groups, with all groups euglycemic (data not shown).

Oil red O staining of frozen livers harvested from fasted $SCAD^{-/-}$ mice, 10 weeks postinjection of PBS, presented the microvesicular fatty change reported by Wood and coworkers (1989) and Armstrong and coworkers (1993). A light micrograph of oil red O-stained liver from an $SCAD^{-/-}$ mouse that received PBS is shown in Fig. 5A. Such microsteatosis within the $SCAD^{-/-}$ liver was not observed in fasted mice 10 weeks postinjection of AAV8-mSCAD (Fig. 5B) or in an $SCAD^{+/+}$ C57BL/6 mouse control (Fig. 5C). There was no consistent presentation of microsteatosis in fasted mice that received AAV5 vector expressing murine SCAD (data not shown).

MRS was performed on $SCAD^{-/-}$ mice that received either AAV8-mSCAD ($n = 4$) or PBS ($n = 4$) 10 weeks postinjection. In addition, four 18-week-old C57BL/6 mice were also scanned to gauge whether rAAV8-mSCAD-mediated expression of SCAD in the liver could reduce the hepatic lipid content to wild-type levels. All mice were fasted overnight before scanning. Magnetic resonance imaging allowed for selection of homogeneous areas within the mouse livers for MRS (Fig. 6A). All MR spectra shown in Fig. 6 were obtained without water suppression. Figure 6B illustrates a magnetic resonance spectrum from an $SCAD^{-/-}$ mouse that received PBS. The major peak represents water and the other peak corresponds to lipid. Figure 6C represents an MR spectrum of a liver from an $SCAD^{-/-}$ mouse that received AAV8-mSCAD vector. A dramatic reduction in the MRS lipid peak was achieved 10 weeks postinjection of AAV8-mSCAD, with the MRS trace comparable to the minimal hepatic fat content observed in $SCAD^{+/+}$ C57BL/6 mice (Fig. 6D). Area integration for the lipid peaks from water-suppressed spectra was determined and assigned arbitrary units. Because the water peak values are constant, a ratio of lipid to water was used to determine the relative lipid content within the liver (Fig. 6E). The mean ratio of lipid to water peaks in $SCAD^{-/-}$ mice that received AAV8-mSCAD was 13-fold lower than the mean ratio of those mice that received PBS, indicating a significant reduction in the relative lipid content within livers that expressed the exogenous SCAD enzyme ($p = 0.039$). In addition, the lipid-to-water value in AAV8-mSCAD-treated mice is at a similar level to that determined in C57BL/6 mice, in which there is only negligible lipid within the liver.

Discussion

The work presented here demonstrates the initial proof-of-concept of AAV8-mediated SCAD gene therapy in the liver of the SCAD-deficient mouse model. Immunoblotting of mitochondrial extracts and immunostaining of liver sections allowed for detection of AAV8 vector-mediated SCAD expression, and significantly increased levels of SCAD en-

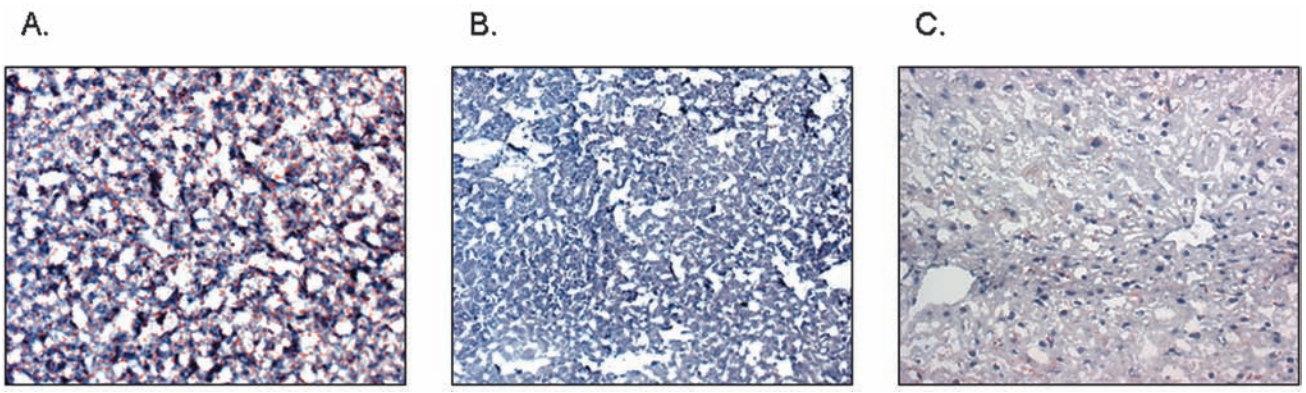

FIG. 5. Oil red O staining of $SCAD^{-/-}$ livers 10 weeks postinjection of AAV8-mSCAD or PBS, via the portal vein. (**A**) Liver section from an $SCAD^{-/-}$ mouse that received PBS via the portal vein. (**B**) Liver section from an $SCAD^{-/-}$ mouse that received 1×10^{11} VG of rAAV8-mSCAD. (**C**) Liver section from a C57BL/6 mouse acting as wild-type control. (**A–C**) Original magnification, ×20.

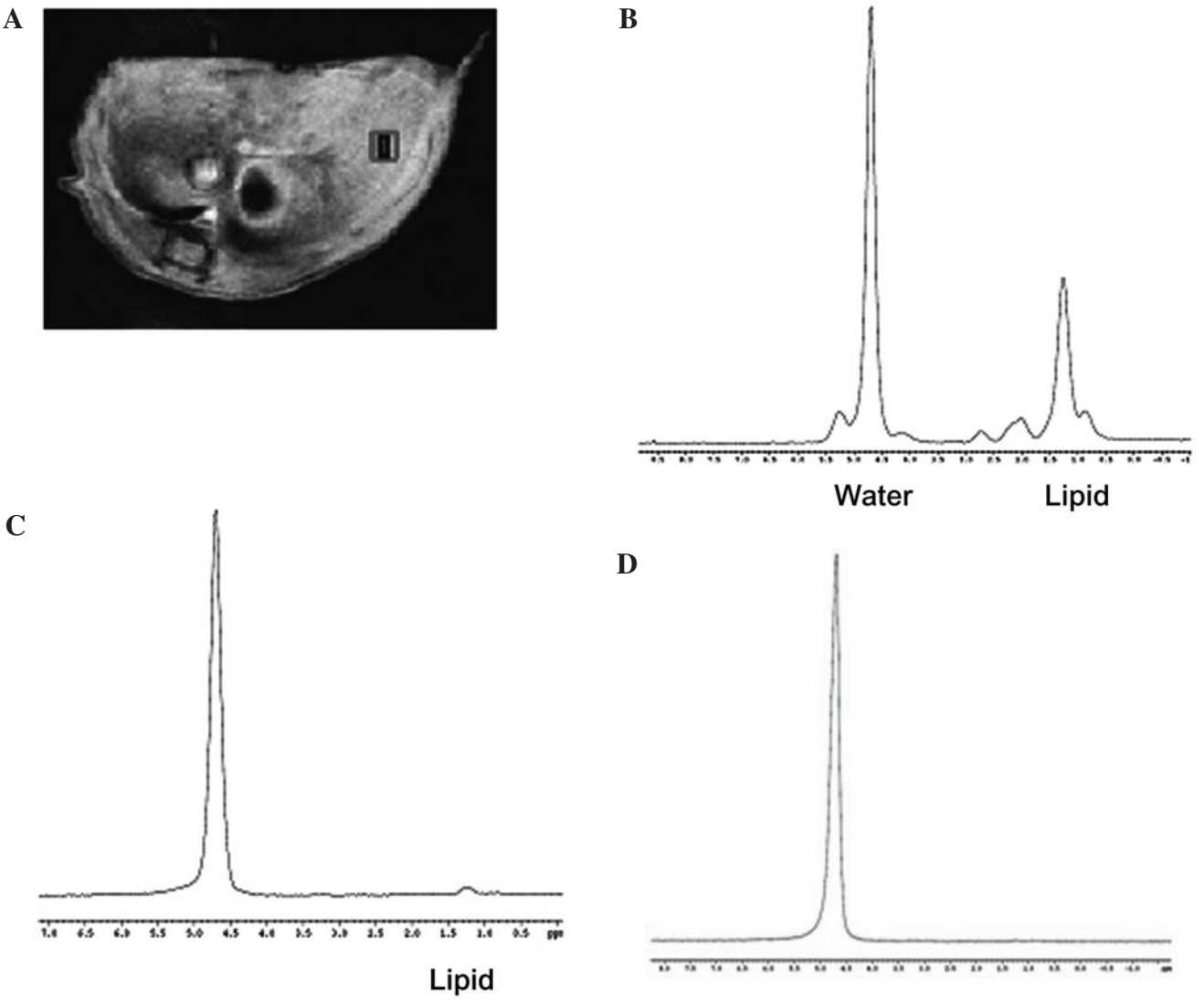

FIG. 6. Decrease in tissue lipid concentrations as demonstrated by proton magnetic resonance spectroscopy 10 weeks after injection of AAV8-mSCAD. (**A**) Single magnetic resonance image of the $SCAD^{-/-}$ mouse liver, used to guide acquisition of the proton magnetic resonance spectrum. The boxed area indicates the location of the voxel from which the proton spectrum was acquired. (**B**) Magnetic resonance spectrum (without water suppression) from an $SCAD^{-/-}$ mouse that received PBS. The water and lipid peaks are indicated. (**C**) Magnetic resonance spectrum (without water suppression) from an $SCAD^{-/-}$ mouse that received AAV8-mSCAD. (**D**) Magnetic resonance spectrum (without water suppression) from a wild-type C57BL/6 mouse. (**E**) Lipid peak value divided by water peak value in livers of SCAD-deficient mice 10 weeks postinjection of 1×10^{11} vg of rAAV8-mSCAD or PBS via the hepatic portal vein. Columns and error bars represent means and SEs, respectively. PBS ($n = 4$); rAAV8 ($n = 4$); C57BL/6 ($n = 4$). *$p < 0.05$.

zyme activity in the liver were demonstrated (~43% that of wild type). Serum butyrylcarnitine profiles and reduced hepatic lipid content, as determined by MRS, both demonstrated biochemical correction of SCAD deficiency after portal vein injection of AAV8-mSCAD. Ten weeks postinjection, immunostaining of liver sections illustrated reduced levels of hepatic SCAD expression in AAV5-treated mice, where ~1–2% hepatocytes stained positive, compared with ~5% in those that received AAV8 vector. Similarly, SCAD-specific antibodies were able to detect SCAD in mitochondrial iso-

lates from livers that received AAV8 but not in those that received AAV5. There was also significantly higher SCAD activity in livers that received AAV8 than AAV5, 10 weeks postinjection.

Recombinant AAV vectors with pseudotype 5 and 8 capsids have been shown to be capable of stable gene transfer and hepatic expression after liver-directed administration (Mingozzi *et al*., 2002; Nakai *et al*., 2005). The tissue tropism and transduction efficiency depend on capsid amino acids, which control initial receptor attachment and/or entry requirements. AAV5 is distantly related to other known AAVs, sharing 54–56% sequence homology (Bantel-Schaal *et al*., 1999). Despite AAV5 having a surface topology similar to that of AAV2, the receptors mediating AAV5 transduction are distinct; for example, one receptor for AAV5 is the platelet-derived growth factor receptor (Pasquale *et al*., 2003). In addition, AAV5 transduction requires binding of α2,3-N-linked sialic acid and, unlike AAV2, transduction is not inhibited by soluble heparin (Kaludov *et al*., 2001; Walters *et al*., 2001). AAV8 is an isolate from rhesus monkey tissue and shows high homology to other AAVs, including 84% homology to AAV2, but has no affinity for heparin sulfate (Lochrie *et al*., 2006). The structure of AAV8 has been determined by Nam and coworkers (2007). Increased AAV8-SCAD transduction compared with AAV5 is in accordance with data obtained after hepatic portal vein injection of various serotype rAAV vectors that express human α_1-antitrypsin in C57BL/6 mice, in which supraphysiologic levels of hAAT were observed out to the end of the study, at 24 weeks (Conlon *et al*., 2005). Indeed, AAV8 has been reported to transduce hepatocytes far more efficiently than other rAAVs tested so far (Gao *et al*., 2002; Nakai *et al*., 2005).

At 4 and 6 weeks postinjection of both AAV5- and AAV8-mSCAD vector groups, circulating butyrylcarnitine levels were significantly reduced compared with levels in SCAD$^{-/-}$ mice that received PBS. This may indicate that hepatic expression of SCAD may be at similar levels for both vector groups at these time points. AAV8 is reported to transduce muscle and heart of adult mice and hamsters, in addition to efficiently transducing the liver after intravenous injection (Wang *et al*., 2005), and rAAV8-mSCAD may have transduced heart and muscle of SCAD$^{-/-}$ mice after portal vein administration. Although AAV5 has not been reported to transduce muscle after intravenous injection, it is feasible that AAV5-mSCAD transduced other tissues in addition to the liver. Such tissues would likely include the lung (Zabner *et al*., 2000; Sumner-Jones *et al*., 2006) and other tissues that display platelet-derived growth factor receptor and α2,3-N-linked sialic acid for binding and transduction of AAV5. ESI-MS/MS data from sera collected 8 and 10 weeks postinjection were unavailable. However, MRS indicated a significant reduction in lipid composition of livers 10 weeks postinjection of AAV8-mSCAD. Indeed, by transducing $\geq$5% hepatocytes with AAV8 vector and producing approximately half the levels of active SCAD enzyme found in wild-type mice, the hepatic lipid content within the SCAD$^{-/-}$ mouse was normalized to C57BL/6 levels. Ongoing studies will determine a dose–response relationship between the AAV8-mSCAD vector, clearance of butyrylcarnitine metabolites, and lipid content within the liver.

Recombinant AAV-mediated delivery of the murine SCAD gene was previously demonstrated in the TA muscle of SCAD$^{-/-}$ mice (Conlon *et al*., 2006). Intramuscular injection of rAAV-mSCAD vector with a pseudotype 1 capsid led to decreased levels of circulating butyrylcarnitine 10 weeks postinjection. Furthermore, MRS of the injected TA leg muscle demonstrated a significant reduction in the lipid peak compared with that of the untreated leg. The reduction in circulating butyrylcarnitine levels suggests that the AAV1-mSCAD-treated TA muscle served as a metabolic sink for excess circulating C_4 metabolites. Despite these promising findings, skeletal muscle may not act as a suitable metabolic sink for longer chain fatty acids, as injection of rAAV1 expressing murine long-chain acyl-CoA dehydrogenase (LCAD) into TA muscle of LCAD-deficient mice did not result in a reduction of circulating long-chain acylcarnitines (our unpublished data). TA muscle, which was chosen because of its accessibility for injection in the mouse, is white fast-twitch muscle rather than red mitochondria-rich slow-twitch muscle, and normally oxidizes few fatty acids for energy. Long-chain fatty acids and acylcarnitines are much more hydrophobic than butyrylcarnitine and may not enter TA muscle as readily for oxidation. In contrast, the liver is a central processing center for long-chain fatty acids, and delivering rAAV vectors expressing the acyl-CoA dehydrogenase to the liver represents a more viable approach towards achieving substantial whole-body changes. SCAD gene delivery to the liver in this study has further demonstrated how MRS of liver acts as a noninvasive, clinically applicable end point for fatty acid oxidation gene replacement therapy.

Disorders of mitochondrial fatty acid β-oxidation may have serious clinical consequences. The disease phenotypes are complex and highly variable, ranging from mild to severe episodes of metabolic decompensation, often presenting as a recurrent Reye's syndrome-like disorder (hypoglycemia, hyperammonemia, and hepatosteatosis) or resulting in sudden unexpected death (Wood, 1999). The data presented here provide further evidence for using recombinant AAV vectors as part of a gene replacement strategy for patients with ACAD deficiencies. From a study of 31 Dutch patients with SCADD, van Maldegem and coworkers (2006) noted that SCADD was not clinically severe and that it was not possible to differentiate diseased from nondiseased individuals (van Maldegem *et al*., 2006). Atypical presentation has, however, been reported, including two infants with SCADD, one who displayed early-onset severe axonal neuropathy and another who presented with brain malformation and infantile spasms (Kurian *et al*., 2004; Mikati *et al*., 2007). SCADD is relatively rare compared with MCAD and VLCAD deficiencies (Liebig *et al*., 2006); however, SCAD gene replacement does act as a surrogate model for MCAD and VLCAD deficiencies, which are clinically relevant. As judged by tandem mass spectrometry blood spot screening of 8.25 million screened newborns, the incidence of MCAD deficiency is 1:14,600 (Rhead, 2006). Since introduction of neonatal screening programs for VLCAD deficiency, the apparent incidence has increased and is now estimated at 1:50,000 to 1:120,000 (Spierkerkoetter *et al*., 2003; Wilcken *et al*., 2003). All together, this study warrants further investigation into liver-directed gene replacement of MCAD and VLCAD, using AAV8 vectors.

Acknowledgments

The authors acknowledge the efforts of the University of Florida Vector Core, and of Tina Yanchis-Kirby (University of Florida Molecular Pathology Core). Funding for this research was provided by an NHLBI grant (HL-59412).

Author Disclosure Statement

No competing financial interests exist.

References

Armstrong, D.A., Masiowski, M.L., and Wood, P.A. (1993). Pathologic characterization of short-chain acyl-CoA dehydrogenase deficiency in BALB/cByJ mice. Am. J. Med. Genet. 47, 884–892.

Bantel-Schaal, U., Delius, H., Schmidt, R., and Zur Hausen, H. (1999). Human adeno-associated virus type 5 is only distantly related to other known primate helper-dependent parvoviruses. J. Virol. 73, 939–947.

Bhala, A., Willi, S.M., Rinaldo, P., Bennett, M.J., Schmidt-Sommerfeld, E., and Hale, D.E. (1995). Clinical and biochemical characterization of short-chain acyl-coenzyme A dehydrogenase deficiency. J. Pediatr. 126, 910–915.

Bradford, M.M. (1976). A rapid and sensitive method for the quantitation of microgram quantities of protein utilizing the principle of protein-dye binding. Anal. Biochem. 72, 248–254.

Conlon, T., Walter, G., Owen, R., Cossette, T., Erger, K., Gutierrez, G., Goetzman, E., Matern, D., Vockley, J., and Flotte, T.R. (2006). Systemic correction of a fatty acid oxidation defect by intramuscular injection of a recombinant adeno-associated virus vector. Hum. Gene Ther. 17, 71–80.

Conlon, T.J., Cossette, T., Erger, K., Choi, Y.K., Clarke, T., Scott-Jorgensen, M., Song, S., Campbell-Thompson, M., Crawford, J., and Flotte, T.R. (2005) Efficient hepatic delivery and expression from a recombinant adeno-associated virus 8 pseudotyped α_1-antitrypsin vector. Mol. Ther. 12, 867–875.

Corydon, M.J., Vockley, J., Rinaldo, P., Rhead, W.J., Kjeldsen, M., Winter, V., Riggs, C., Babovic-Vuksanovic, D., Smeitink, J., De Jong, J., Levy, H., Sewell, A.C., Roe, C., Matern, D., Dasouki, M., and Gregersen, N. (2001). Role of common gene variations in the molecular pathogenesis of short-chain acyl-CoA dehydrogenase deficiency. Pediatr. Res. 49, 18–23.

Frerman, F.E., and Goodman, S.I. (1985). Fluorometric assay of acyl-CoA dehydrogenases in normal and mutant human fibroblasts. Biochem. Med. 33, 38–44.

Gao, G.P., Mauricio, R., Alvira, M.R., Wang, L., Calcedo, R., Johnston, J., and Wilson, J.M. (2002). Novel adeno-associated viruses from rhesus monkeys as vectors for gene therapy. Proc. Natl. Acad. Sci. U.S.A. 99, 11854–11859.

Gregersen, N., Winter, V.S., Corydon, M.J., Corydon, T.J., Rinaldo, P., Ribes, A., Martinez, G., Bennett, M.J., Vianey-Saban, C., Bhala, A., Hale, D.E., Lehnert, W., Kmoch, S., Roig, M., Riudor, E., Eiberg, H., Andresen, B.S., Bross, P., Bolund, L.A., and Kølvraa, S. (1998). Identification of four new mutations in the short-chain acyl-CoA dehydrogenase (SCAD) gene in two patients: One of the variant alleles, 511C → T, is present at an unexpectedly high frequency in the general population, as was the case for 625G → A, together conferring susceptibility to ethylmalonic aciduria. Hum. Mol. Genet. 7, 619–627.

Holm, D.A., Dagnës-Hansen, F., Simonsen, H., Gregersen, N., Bolund, L., Jensen, T.G., and Corydon, T.J. (2003). Expression of short-chain acyl-CoA dehydrogenase (SCAD) proteins in the liver of SCAD deficient mice after hydrodynamic gene transfer. Mol. Genet. Metab. 78, 250–258.

Kaludov, N., Brown, K.E., Walters, R.W., Zabner, J., and Chiorini, J.A. (2001). Adeno-associated virus serotype 4 (AAV4) and AAV5 both require sialic acid binding for hemagglutination and efficient transduction but differ in sialic acid linkage specificity. J. Virol. 75, 6884–6893.

Kelly, C.L., Rhead, W.J., Kutschke, W.K., Brix, A.E., Hamm, D.A., Pinkert, C.A., Lindsey, J.R., and Wood, P.A. (1997).Functional correction of short-chain acyl-CoA dehydrogenase deficiency in transgenic mice: Implications for gene therapy of human mitochondrial enzyme deficiencies. Hum. Gene Ther. 6, 1451–1455.

Kurian, M.A., Hartley, L., Zolkipli, Z., Little, M.A., Costigan, D., Naughten, E.R., Olpin, S., Muntoni, F., and King, M.D. (2004). Short-chain acyl-CoA dehydrogenase deficiency associated with early onset severe axonal neuropathy. Neuropediatrics 35, 312–316.

Liebig, L., Schymik, I., Mueller, M., Wendel, U., Mayatepek, E., Ruiter, J., Strauss, A.W., Wanders, R.J.A., and Spiekerkoetter, U. (2006). Neonatal screening for very long-chain acyl-CoA dehydrogenase deficiency: Enzymatic and molecular evaluation of neonates with elevated $C_{14:1}$-carnitine levels. Pediatrics 118, 1065–1069.

Lochrie, M.A., Tatsuno, G.P., Christie, B., Wellman McDonnell, J., Zhou, S., Surosky, R., Pierce, G.F., and Colosi, P. (2006). Mutations on the external surfaces of adeno-associated virus type 2 capsids that affect transduction and neutralization. J. Virol. 80, 821–834.

Mikati, M., Chaaban, H.R., Karam, P.E., and Krisnamoorthy, K.S. (2007). Brain malformation and infantile spasms in a SCAD deficiency patient. Pediatr. Neurol. 36, 48–50.

Mingozzi, F., Schuttrumpf, J., Arruda, V.R., Liu, Y., Liu, Y.L., High, K.A., Xiao, W., and Herzog, R.W. (2002). Improved hepatic gene transfer by using an adeno-associated virus serotype 5 vector. J. Virol. 76, 10497–10502.

Nagan, N., Kruckeberg, K.E., Tauscher, A.L., Bailey, K.S., Rinaldo, P., and Matern, D. (2003). The frequency of short-chain acyl-CoA dehydrogenase gene variants in the US population and correlation with the C_4-acylcarnitine concentration in newborn blood spots. Mol. Genet. Metab. 78, 239–246.

Naito, E., Ozasa, H., Ikeda, Y., and Tanaka, K. (1989). Molecular cloning and nucleotide sequence of complementary DNAs encoding human short chain acyl-coenzyme A dehydrogenase and the study of the molecular basis of human short chain acyl-coenzyme A dehydrogenase deficiency. J. Clin. Invest. 83, 1605–1613.

Naito, E., Indo, Y., and Tanaka, K. (1990). Identification of two variant short chain acyl-coenzyme A dehydrogenase alleles, each containing a different point mutation in a patient with short chain acyl-coenzyme A dehydrogenase deficiency. J. Clin. Invest. 85, 1575–1582.

Nakai, H., Fuess, S., Storm, T.A., Muramatsu, S., Nara, Y., and Kay, M.A. (2005). Unrestricted hepatocyte transduction with adeno-associated virus serotype 8 vectors in mice. J. Virol. 79, 214–224.

Nam, H.J., Lane, M.D., Padron, E., Gurda, B., McKenna, R., and Kohlbrenner, E. (2007). Structure of adeno-associated virus serotype 8, a gene therapy vector. J. Virol. 81, 12260–12271.

Pasquale, G.D., Davidson, B.L., Stein, C.S., Martins, I., Scudiero, D., and Monks, A. (2003). Identification of PDGFR as a receptor for AAV-5 transduction. Nat. Med. 10, 1306–1312.

Rhead, W. (2006). Newborn screening for medium-chain acyl-CoA dehydrogenase deficiency: A global perspective [review]. J. Inherit. Metab. Dis. 29, 370-377.

Ribes, A., Riudor, E., Garavaglia, B., Martinez, G., Arranz, G., Invernizzi, F., Briones, P., Lamantea, E., Sentis, M., Barcelo,

A., and Roig, M. (1998). Mild or absent clinical signs in twin sisters with short-chain acyl-CoA dehydrogenase deficiency. Eur. J. Pediatr. 157, 317–320.

Rinaldo, P., and Matern, D. (2005). Inborn errors of amino acid, organic acid, and fatty acid metabolism. In: C.A. Burtis, E.R. Ashwood, and N.W. Tietz, eds. *Tietz Textbook of Clinical Chemistry*, 4th ed. (W.B. Saunders, Philadelphia) pp. 2207–2247.

Seidel, J., Streck, S., Bellstedt, K., Vianey-Saban, C., Pedersen, C.B., Vockley, J., Korall, H., Roskos, M., Deufel, T., Trefz, K.F., Sewell, A.C., Kauf, E., Zintl, F., Lehnert, W., and Gregersen, N. (2003). Recurrent vomiting and ethylmalonic aciduria associated with rare mutations of the short-chain acyl-CoA dehydrogenase gene. J. Inherit. Metab. Dis. 26, 37–42.

Spierkerkoetter, U., Sun, B., Zytkovicz, T., Wanders, R., Strauss, A.W., and Wendel, U. (2003). MS/MS-based newborn and family screening detects asymptomatic patients with very long-chain acyl-CoA dehydrogenase deficiency. J. Pediatr. 143, 335–342.

Sumner-Jones, S.G., Davies, L.A., Varathalingam, A., Gill, D.R., and Hyde, S.C. (2006). Long-term persistence of gene expression from adeno-associated virus serotype 5 in the mouse airways. Gene Ther. 13, 1703–1713.

Tein, I., Elpeleg, O., Ben-Zeev, B., Korman, S.H., Lossos, A., Lev, D., Lerman-Sagie, T., Leshinsky-Silver, E., Vockley, J., Berry, G.T., Lamhonwah, A.M., Matern, D., Roe, C.R., and Gregersen, N. (2008). Short-chain acyl-CoA dehydrogenase gene mutation (c.319C>T) presents with clinical heterogeneity and is candidate founder mutation in individuals of Ashkenazi Jewish origin. Mol. Genet. Metab. 93, 179–189.

van Maldegem, B.T., Duran, M., Wanders, R.J., Niezen-Koning, K.E., Hogevenn, M., Ijlst, L., Waterham, H.R., and Wijburg, F.A. (2006). Clinical, biochemical, and genetic heterogeneity in short-chain acyl-coenzyme A dehydrogenase deficiency. JAMA 296, 943–952.

Walters, R.W., Yi, S.M., Keshavjee, S., Brown, K.E., Welsh, M.J., Chiorini, J.A., and Zabner, J. (2001). Binding of adeno-associated virus type 5 to 2,3-linked sialic acid is required for gene transfer. J. Biol. Chem. 276, 20610–20616.

Wang, Z., Zhu, T., Qiao, C., Zhou, L., Wang, B., Zhang, J., Chen, C., and Xiao, X. (2005). Adeno-associated virus serotype 8 efficiently delivers genes to muscle and heart. Nat. Biotechnol. 23, 321–328.

Wilcken, B., Wiley, V., Hammond, J., and Carpenter, K. (2003). Screening newborns for inborn errors of metabolism by tandem mass spectrometry. N. Engl. J. Med. 384, 2304–2312.

Wood, P.A. (1999). Defects in mitochondrial β-oxidation of fatty acids. Curr. Opin. Lipidol. 10, 107–112.

Wood, P.A., Amendt, B.A., Rhead, W.J., Millington, D.S., Inoue, F., and Armstrong, D. (1989). Short-chain acyl-coenzyme A dehydrogenase deficiency in mice. Pediatr. Res. 25, 38–43.

Xu, L., Daly, T., Gao, C., Flotte, T.R., Song, S., Byrne, B.J., Sands, M.S., and Ponder, K.P. (2001). CMV-β-actin promoter directs higher expression from an adeno-associated viral vector in the liver than the cytomegalovirus or elongation factor 1α promoter and results in therapeutic levels of human factor X in mice. Hum. Gene Ther. 12, 563–573.

Zabner, J., Seiler, M., Walters, R., Kotin, R.M., Fulgeras, W., Davidson, B.L., and Chiorini, J.A. (2000). Adeno-associated virus type 5 (AAV5) but not AAV2 binds to the apical surfaces of airway epithelia and facilitates gene transfer. J. Virol. 74, 3852–3858.

Zolotukhin, S., Potter, M., Zolotukhin, I., Sakai, Y., Loiler, S., Fraites, T.J., Jr., Chiodo, V.A., Phillipsberg, T., Muzyczka, N., Hauswirth, W.H., Flotte, T.R., Byrne, B.J., and Snyder, R.O. (2002). Production and purification of serotype 1, 2, and 5 recombinant adeno-associated viral vectors. Methods 28, 158–167.

Address reprint requests to:
Dr. T.R. Flotte
Dean's Office, Medical School
University of Massachusetts
Room S1-340
55 Lake Avenue North
Worcester, MA 01655

E-mail: Terry.Flotte@umassmed.edu

Received for publication December 7, 2007; accepted after revision March 17, 2008.

Published online: May 27, 2008.